Available online at www.sciencedirect.com

SCIENCE DIRECT®

ELSEVIER

Computers and Electronics in Agriculture 51 (2006) 86–98

Computers and electronics in agriculture

www.elsevier.com/locate/compag

Using digital image analysis and spectral reflectance data to quantify damage by greenbug (Hemitera: Aphididae) in winter wheat

M. Mirik[a,*], G.J. Michels Jr.[a], S. Kassymzhanova-Mirik[a], N.C. Elliott[b], V. Catana[b], D.B. Jones[c], R. Bowling[d]

[a] *Texas A&M University System, Agricultural Research and Extension Center, 6500 Amarillo Blvd. West, Amarillo, TX 79106, USA*
[b] *USDA-ARS, 1301 N. Western Road, Stillwater, OK 74075, USA*
[c] *Department of Entomology and Plant Pathology, 127 Noble Research Center, Oklahoma State University, Stillwater, OK 74078, USA*
[d] *Pioneer Sales and Marketing, 501 Pine Ave., Dumas, TX 79029, USA*

Received 7 September 2005; received in revised form 21 November 2005; accepted 28 November 2005

Abstract

The usefulness of digital image analysis and spectral reflectance data to quantify damage by greenbugs (*Schizaphis graminum* (Rondani)) was evaluated for two winter wheat (*Triticum aestivum* L.) fields, three field experiments, and one greenhouse experiment in Oklahoma and Texas. A hyperspectral field spectrometer and a digital camera were used to record reflectance and to acquire images over 0.25-, 0.37-, and 1-m^2 greenbug-damaged wheat canopies. A large number of spectral vegetation indices compiled from the literature were calculated and relationship to damage by greenbugs was investigated. The mean percent damage by greenbugs estimated through digital image analysis varied from $13 \pm 1/0.25$ to $73 \pm 7/0.37\ m^2$. The mean greenbug abundance ranged from $191 \pm 22/0.25$ to $54{,}209 \pm 7908/0.37\ m^2$. Correlation analyses showed strong associations between damage by greenbugs in wheat and spectral vegetation indices. Correlation coefficient ranged from 0.82 to −0.98. These results suggest that remote sensing using spectral reflectance and digital images can be nondestructive, rapid, cost-effective, and reproducible techniques to determine damage by greenbugs in wheat with repeatable accuracy and precision. Together with the existing spectral indices, two versions of a new index algorithm are suggested in this paper.

Keywords: Digital image; Greenbug (*Schizaphis graminum* (Rondani)); Spectral reflectance; Remote sensing; Vegetation indices; Wheat (*Triticum aestivum* L.)

1. Introduction

To implement timely control strategies through plant monitoring, an accurate quantification of disease and damage caused by biotic and abiotic stressors in plants is required. Currently, visual disease and damage quantification methods are the most common (Horst et al., 1984; Richardson et al., 2001; Guan and Nutter, 2002; Steddom et al., 2004, 2005b) but these techniques are subject to bias and can be inaccurate (Sherwood et al., 1983; Nutter et al., 1993; Nilsson, 1995; Richardson et al., 2001; Turner et al., 2004). Imprecise and inaccurate data may cause costly errors when

* Corresponding author. Tel.: +1 806 354 5834; fax: +1 806 354 5829.
E-mail address: MMirik@ag.tamu.edu (M. Mirik).

0168-1699/$ – see front matter © 2006 Elsevier B.V. All rights reserved.
doi:10.1016/j.compag.2005.11.004

management and policy decisions are based on biased damage evaluation (Raikes and Burpee, 1998). For example, subjective quantifications of leaf spot in a turfgrass (*Poa pratensis* L.) made by 14 observers in a single day ranged two- to three-fold (Skogley and Sawyer, 1992). Nutter et al. (1993) observed significant variation among raters when dollar spot severity was visually assessed in creeping bentgrass (*Agrostis stolonifera* var. *palustris* Farwell), but spectral reflectance measured with a radiometer from the same experiment exhibited greater precision. Disease and damage quantifications in plants during a growing season, even by a single observer, are likely to be inconsistent and not readily comparable (Trenholm et al., 1999; Karcher and Richardson, 2003; Turner et al., 2004). Differences in assessments by humans occur because individuals differ in their capability to perceive various wavelengths of visible light, which can lead to differences in visual estimates of disease severity. Fatigue, lack of concentration and experience, and bias among the observers, such as underestimates of high levels of disease after assessing low levels or vice versa, increase the subjective nature of visual estimates of disease severity (Nilsson, 1995). Horst et al. (1984) analyzed the results of 10 trained researchers, each of whom subjectively evaluated the same turfgrass stands for quality and density, to establish the uniformity of their ratings. More variation was associated with the individual evaluator than with cultivars rated. Consequently, traditional visual damage and disease quantifications in plants suffer from a lack of accuracy and precision (Horst et al., 1984; Richardson et al., 2001; Nutter et al., 2002; Karcher and Richardson, 2003; Steddom et al., 2004).

An alternative method that is consistent, unbiased, and precise is computer automated digital image analysis (Steddom et al., 2004; Turner et al., 2004). Computerized digital image analysis is also a nondestructive and non-invasive method that can capture, process, and analyze information from images (Richardson et al., 2001; Díaz-Lago et al., 2003; Karcher and Richardson, 2003). Current image collection equipment and image analysis programs offer the possibility to acquire hundreds of quality images per hour, which can be analyzed later with a great degree of automation at the observer's convenience (Díaz-Lago et al., 2003). Additionally, digital images can be stored and used as historical archives of vegetation status for a possible future application. Readily available, inexpensive computers, cameras, scanners, and software packages make this method attractive at the present time (Steddom et al., 2004). Steddom et al. (2005a) characterized the importance of image analysis for plant pathology with the phrase "a picture is worth a thousand words."

Digital image analysis has been used in several studies to quantify disease, stress, coverage, and color (Richardson et al., 2001; Sherwood et al., 1983; Adamsen et al., 1999; Díaz-Lago et al., 2003; Diéguez-Uribeondo et al., 2003; Karcher and Richardson, 2003; Steddom et al., 2004). All these studies concluded that digital image analysis is very useful to quantify biophysical plant parameters, for example, working with wheat leaf rust and tan spot on wheat leaves (*Triticum aestivum* L.). Steddom et al. (2004) determined the impacts of sample size, image size, format, and quality on digital image analysis results covering a range of disease intensity. The authors concluded that digital image analyses, even using low-quality Joint Photographers Expert Group (JPEG) images, have a number of desirable qualities for disease quantification because they are very robust and amenable to low-cost, commercially available equipment.

In addition to digital image analysis, an alternative method is to measure the reflectance from the vegetation surface. Reflectance data also provide accurate and precise damage quantification in plants (Nilsson and Johnsson, 1996; Riedell and Blackmer, 1999; Yang et al., 2005). A common method proven to be functional is the transformation of reflectance data into vegetation indices. Hence, many spectral vegetation indices have been proposed because they exhibit high correlations with the ecological variables collected in dissimilar environments. An attractive feature of spectral vegetation indices is the ability to factor out the effects of noise or disturbance factors in relation to reflectance and characteristics of the target objects. Undesirable noise or disturbance factors include differences in plant species, canopy coverage, soil background, atmospheric condition, illumination, shadowing, solar angle, and viewing geometry of the recording device over time and space (Bouman, 1995; Yoshioka et al., 2000).

Perhaps the most widely used and best known indices are those that combine near-infrared (NIR) and red light in their construction. Examples of these type of indices are the Normalized Difference Vegetation Index $(\mathrm{NDVI}) = (\mathrm{NIR_{band}} - \mathrm{RED_{band}})/(\mathrm{NIR_{band}} + \mathrm{RED_{band}})$ developed by Rouse et al. (1973) and simple ratio $(\mathrm{SR}) = \mathrm{NIR_{band}}/\mathrm{RED_{band}}$ proposed by Jordan (1969). Many other indices have been designed using different or rearranged wavebands to diagnose the changes in plant phenology and physiology. Some of these spectral indices are the Moisture Stress Index (Hunt and Rock, 1989), Water Deficit Index (Moran et al., 1994), Normalized Difference Water Index (Gao, 1996), Plant Senescing Reflectance Index (Merzlyak et al., 1999), Normalized Difference Nitrogen and Lignin Indices (Serrano et al., 2002), Global Vegetation Moisture Index (Ceccato et al., 2002), Shortwave Infrared

Water Stress Index (Fensholt and Sandholt, 2003), and Nitrogen Stress Index (Kruse et al., 2004). As the names suggest, these indices basically aim to measure stresses caused by abiotic stressors, mainly water and nitrogen.

Many studies have concluded that the use of remote sensing, and, in turn, vegetation indices, has been an effective technique for detecting stress in plants. Bawden (1933) was the first to use aerial photography to detect plant viruses in tobacco (*Nicotiana tabacum* L.) and potato (*Solanum tuberosum* L.). Subsequently, spectral data have been used to detect stress in shortleaf pine (*Pinus echinata* Mill.) (Carter et al., 1998), jack pine (*Pinus banksiana* Lamb.) (Leckie et al., 2005), sugar beet (*Beta vulgaris* L.) (Steddom et al., 2003, 2005b; Laudien et al., 2004), rice (*Oryza sativa* L.) (Kobayashi et al., 2001; Qin and Zhang, 2005), creeping bentgrass (Raikes and Burpee, 1998), alfalfa (*Medicago sativa* L.) (Guan and Nutter, 2002), peanut (*Arachis hypogaea* L.) (Aquino et al., 1992; Nutter and Littrell, 1996), field bean (*Vicia faba* L.) (Malthus and Madeira, 1993), watermelon (*Citrullus vulgaris* Schrad.) (Blazquez and Edwards, 1986), tomato (*Lycopersicon esculentum* L.) (Zhang et al., 2003), cotton (*Gossypium hirsutum* L.) (Toler et al., 1981; Read et al., 2002), sunflower (*Helianthus annuus* L.) (Mariotti et al., 1996), soybean (*Glycine max* L.) (Adams et al., 2000), maize (*Zea mays* L.) (Kim et al., 2000), barley (*Hordeum vulgare* L.) (Nilsson and Johnsson, 1996; Peñuelas et al., 1997; Newton et al., 2004), and wheat (Lelong et al., 1998; Muhammed and Larsolle, 2003; Jones, 2004; Muhammed, 2004). In addition, Riedell and Blackmer (1999) and Yang et al. (2005) used remote sensing to characterize damage by greenbug (*Schizaphis graminum* (Rondani)) in controlled conditions and concluded that vegetation indices were able to characterize damage by greenbugs in wheat.

The usefulness of remote sensing to characterize stress in plants has long been established although the potential use of this method to quantify damage by greenbugs in wheat at the canopy level has not yet been documented. This implies need for remote sensing research to quantify damage by greenbugs in real-time field situations because widespread or localized infestations by greenbug frequently reach damaging levels and cause severe damage to wheat. The greenbug is viewed as one of the most destructive insects of wheat in the Great Plains region of the United States (US). Wheat production losses caused by greenbug in wheat for the US economy were estimated to be from US$ 60 M to more than 100 M annually (Webster et al., 2000).

With the ability to detect stress, estimated damage severity through digital image analysis and spectral vegetation indices can be combined to quantify damage by greenbugs in wheat. This combination presents an unbiased, nondestructive, and rapid damage quantification method that can be used to monitor the health of the wheat crop at a single or at multiple times during a growing season. This combination also has the benefit of excluding the experimental and evaluator errors, leaving only instrumental errors inherent in instrument design. The present research is a continuation of a previous study (Mirik, unpublished data). The earlier work was successful in identifying differences in spectral reflection patterns of greenbug-infested and noninfested winter wheat canopies and revealing a high correlation between greenbug abundance and spectral vegetation indices. A logical next step was to examine the correlations between spectral data and damage by greenbugs. Therefore, the objective of the present study was to evaluate the relationship between spectral vegetation indices and damage by greenbugs estimated through digital image analysis in wheat.

2. Materials and methods

2.1. Field locations and greenhouse experiment

Data were collected in two wheat fields in Texas, three wheat fields in Oklahoma, and a greenhouse experiment in Texas (Table 1). Two Texas wheat fields infested by greenbug were monitored in the fall of 2003 and again in the spring of 2005. One volunteer winter wheat field was near Dumas (35°84′N latitude, 101°96′W longitude, and altitude 1098 m) in Moore County, TX (Field 1 hereafter), and the other was a winter wheat field near Chillicothe, TX (34°25′N latitude, 99°49′W longitude, and altitude 410 m), in Hardeman County, TX (Field 2 hereafter). The Oklahoma winter wheat field experiments were located southwest of Oklahoma City: one (Field 3 hereafter) near Chickaska in Grady County and two near Apache (Fields 4 and 5 hereafter) in Caddo County. The latitudes, longitudes, and altitudes were 35°05′N, 97°91′W, and 300 m for Field 3, 34°89′N, 98°46′W, and 403 m for Field 4, 34°88′N, 98°36′W, and 347 m for Field 5 (Table 1). In each field, four, 30 m × 30 m plots were established with a minimum of a 10-m buffer zone between plots. One plot was treated with chlorpyrifos (Lorsban® 4E, Dow AgroSciences, 1.6 l/ha) and imidacloprid (Provada®, Bayer AG, Leverkusen, Germany, 335 g/ha) once a month to remove aphids. The remaining plots were not treated to facilitate infestation by greenbugs. The Oklahoma winter wheat fields were monitored for greenbug once a month. In addition to natural greenbug infestations in fields, a greenhouse experiment using wheat grown in

Table 1
Location, wheat growth stage, sampling date, sample size, sample number, spectrometer, and camera height for five fields and one greenhouse experiments studied

	Field 1	Field 2	Field 3	Field 4	Field 5	GrHs Exp
Latitude	35°84′N	34°25′N	35°05′N	34°89′N	34°88′N	35°19′N
Longitude	101°96′W	99°49′W	97°91′W	98°46′W	98°36′W	102°08′W
Altitude (m)	1098	410	300	403	347	1162
Sampling date	11.21.2003	05.18.2005	11.17.2003	11.18.2003	11.19.2003	05.23.2005
Growth stages (Zadok's scale)	30	32	25	25	25	23
Sample size (m^2)	0.25	1	0.25	0.25	0.25	0.37
Sample number	8	18	24	24	18	10
Spectrometer height (m)	0.65	2.2	0.65	0.65	0.65	0.75
Camera height (m)	1	2	1	1	1	1
State	Texas	Texas	Oklahoma	Oklahoma	Oklahoma	Texas
County	Moore	Hardeman	Grady	Caddo	Caddo	Potter

GrHs Exp – greenhouse experiment.

flats was done at the Texas A&M University Agricultural Experiment Station facilities at Bushland, TX, in the spring of 2005.

2.2. Sampling procedures

In Field 1, eight small patches of greenbug-damaged wheat were located by a ground survey on 21 November 2003 (Table 1). A total of eight samples of size 0.25 m^2 were taken from the greenbug-damaged wheat patches. The wheat crop was at Zadoks' vegetative growth stage 30 (Zadoks et al., 1974). In Field 2, two, 200-m transects (one from north to south and the other west to east) were set up and a total of 18, 1-m^2 greenbug-damaged wheat samples (9 samples for each transect) were established at 20-m intervals on 18 March 2005. The wheat crop was at Zadoks' stage 32. A total of four, 30-m transects at 7-m intervals were set up and 24, 0.25-m^2 sample plots at 5-m intervals were located in one of the nontreated plots in Fields 3–4 on 17–18 December 2003, respectively. Three, 30 m transects at 10 m intervals were established and 18, 0.25-m^2 sample plots at 5 m intervals were located in one of the untreated plots in Field 5 on 19 December 2003. There were six samples along each transect and the wheat crop was at Zadoks' stage 25 in Fields 3–5 (Table 1).

The greenhouse experiment involved two treatments: (1) greenbug-infested and (2) noninfested (check) wheat. There were 10 replications of each treatment. On 10 March 2005, 288 wheat seeds spaced at 2.5 cm × 3.2 cm apart were planted in 20 wooden flats (64 cm × 61 cm × 9 cm) containing field soil as the growth medium. Ten randomly selected flats were put in one greenhouse and the remaining 10 flats were kept in another greenhouse separated by a breezeway. When the wheat was at approximately Zadoks' stage 23, 10 wheat flats were infested with 100 greenbugs/flat in three flats, 200 greenbugs/flat in two flats, 500 greenbugs/flat in three flats, and 700 greenbugs/flat in the remaining two flats. The remaining 10 flats were kept free of greenbugs. Wheat plants in all flats were watered three times per week. Twenty-one days after infesting, flats of both treatments were taken outside the greenhouse to make spectral measurements and take digital images in full sunlight.

2.3. Remote sensing measurements

Spectral measurements were made with an Ocean Optics S2000 hyperspectral hand-held spectrometer (Ocean Optics Inc., Dunedin, FL). Dark current and spectralon readings were taken at the beginning of every 8–10 samples (approximately every 15 min). The spectrometer is a linear, charge-coupled device (CCD)-array detector that collects reflectance data from 339.71 to 1015.52 nm with a continuous spectral resolution ≈0.33 nm. The field of view of the spectrometer is 25°. To reduce the volume of data recorded for each plot by the spectrometer, adjacent wavelengths were initially averaged to 1-nm intervals. To determine optimal band centers and spectral resolutions in relation to damage by greenbugs, the band centers were increased nine times by averaging every 2, 3, . . ., 10 neighboring bands. The hyperspectral spectrometer was mounted to a pole and elevated about 75 cm above the flat surface to collect reflected light from the wheat canopy over 0.37-m^2 sample areas. The same spectral measurements of the wheat canopy were

Fig. 1. Digital images of greenbug (*Schizaphis graminum* (Rondani)) infested (top) and noninfested wheat canopies (bottom) collected near Dumas, Moore County, TX.

used for Fields 1–5 with the exception of spectrometer elevations over the sample plots. Spectrometer elevations were kept about 65 cm to record the reflectance over 0.25-m^2 samples for Fields 1 and 3–5, and 220 cm for Field 2 (Table 1).

Subsequent to the spectral measurements, 0.25- and 1-m^2 frames were placed over each of the scanned samples and high-quality (Tagged Image File Format: TIFF) digital images were taken by a Nikon coolpix5000 digital camera mounted on a pole 100 and 200 cm over and perpendicular to the flats and sample plots to cover areas slightly larger than the 0.37-m^2 for the greenhouse experiment, 0.25-m^2 for Fields 1 and 3–5, and 1-m^2 for Field 2 (Fig. 1; Table 1). Image and reflectance data were collected between 11:30 and 13:30 h to keep the effect of the sun angle the same for all fields and the greenhouse experiment.

2.4. Percentage damage by greenbugs estimated by using ASSESS

All images from Fields 1–5 and the greenhouse experiment were cropped by digitizing the area inside the 0.25- and 1-m^2 frames and 0.37-m^2 flats through ASSESS: Image Analysis Software for Plant Disease Quantification (Lamari, 2002). Cropped images were used to determine the percent damage by greenbugs on leaves. The percent damage by greenbugs was estimated following the methods in the ASSESS user's manual. Masking and thresholding were done using hue saturation intensity (HSI) color space and saturation values on leaves (green coverage). The percent damage by greenbugs was calculated as lesion pixels/leaf pixels × 100%. Color space settings were determined for several images from each field and the greenhouse experiment. The macro facilities of ASSESS were used, as detailed in the tutorial of the user's manual, to process all images from the same field with the same settings, thereby keeping the user's bias to a minimum. Six macro settings, one for each field and the greenhouse experiment, were used to reduce the field and weather variability because soil background and weather conditions varied across the fields and sampling dates. To compare visual rating and digital image analysis, the percent damage by greenbugs was also visually assessed in Fields 2 and the greenhouse experiment.

2.5. Aphid data collection

After acquisition of reflectance data and image, an SH 85 Vacuum/Shredder aspirator (Stihl Inc., Virginia Beach, VA) was used to collect greenbugs from the eight sample plots by placing a screen into the hose of the machine and a 0.25-m^2 heavy metal frame on the ground in Field 1. Collected greenbugs were gently placed with wheat leaves to keep them alive in plastic bags, and transported to the laboratory. Within 24 h of sampling, greenbugs at the laboratory were counted while they were alive. In Field 2 and the greenhouse experiment, 20 tillers were randomly taken inside of each 1-m^2 frame and 0.37-m^2 flat and greenbugs were counted on them. Subsequent to counting greenbugs on 20 tillers, the numbers of wheat tillers within each frame and flat were tallied and greenbug abundance was estimated as: total aphids per frame and flat = (total tillers × total aphids on 20 tillers)/20. A 0.25-m^2 frame was placed on each of the sampling plots to take greenbug density data in Fields 3–5. In Field 3, 12 wheat plants were taken just outside of each plot and greenbugs were counted. On each of the four sides of the plots, greenbugs were counted on 3 wheat plants totaling 12 plants. Subsequent to counting greenbugs on 12 plants, the number of wheat plants within each 0.25-m^2 plot was counted and greenbug abundance determined as: total aphids/0.25 m^2 = (total plants × total aphids on 12 plants)/12. In Field 4, greenbugs were counted in each of 24, 0.25-m^2 plots. In Field 5, greenbugs were counted in each of the first 12 of the 18 plots and the greenbug abundance estimation method used for Field 3 was applied for the remaining 6 plots.

2.6. Spectral index formulation

Various vegetation indices were computed to investigate their correlations with percent damage by greenbugs. Throughout this research, the band centers used to calculate spectral vegetation indices from the literature were sometimes replaced with new wavebands from hyperspectral data to test the wavelengths reported by Riedell and Blackmer (1999) and Yang et al. (2005). Among the vegetation indices tested, the Visible Atmospherically Resistant Index [VARI = $(R_{\text{green}} - R_{\text{red}})/(R_{\text{green}} + R_{\text{red}} - R_{\text{blue}})$] developed by Gitelson et al. (2002) was examined and modified by adding NIR and green wavebands as in the following formula:

$$\frac{(R_i - R_j - R_k - R_l)}{((R_i - R_j) + (R_k - R_l))}$$

Here R_i is the reflectance values or band centers in the ranges between 700 and 900 nm, R_j between 750 and 950 nm but greater than R_i, R_k between 500 and 700 nm, and R_l between 500 and 750 nm but greater than R_k. In the present study, two versions of this index were used. These indices were designated using all possible band combinations available for the given spectral range and their correlations with the percent damage by greenbugs as Damage Sensitive Spectral Index$_1$ and Damage Sensitive Spectral Index$_2$ (DSSI$_1$ and DSSI$_2$).

$$\text{DSSI}_1 = \frac{(R_{719} - R_{873} - R_{509} - R_{537})}{((R_{719} - R_{873}) + (R_{509} - R_{537}))}$$

$$\text{DSSI}_2 = \frac{(R_{747} - R_{901} - R_{537} - R_{572})}{((R_{747} - R_{901}) + (R_{537} - R_{572}))}$$

Table 2
Greenbug (*Schizaphis graminum* (Rondani)) abundance and percentage damage to winter wheat at five field and one greenhouse experiments

	Minimum	Mean	Maximum	S.E.	LCI (0.95)	UCI (0.95)
Field 1						
GD	83	191	286	22	140	243
PGD	27	35	43	2	31	40
Field 2						
GD	156	8603	17376	1411	5625	11580
PGD	7	47	85	5	36	58
VAPGD	42	66	95	4	58	74
Field 3						
GD	291.00	1645.58	4105.00	247.89	1133.00	2158
PGD	10.42	24.00	43.00	2	19	28
Field 4						
GD	61.00	291.25	837.00	41.08	206.00	376
PGD	3.91	13.11	29.08	1.45	10.11	16.11
Field 5						
GD	588.00	2443.17	7202.00	395.00	1611.00	3276
PGD	5	17	25	1	14	19
GrHs Exp						
GD	15120	54209	88387	7908	36320	72099
PGD	39	73	98	7	56	89
VAPGD	20	67	95	9	46	88

Field 1—near Dumas, Moore County, TX, sampled on 21 November 2003. Sample size = 0.25 m^2, n = 8. Field 2—near Chillicothe, Hardeman County, TX, sampled on 18 May 2005. Sample size = 1 m^2, n = 18. Field 3—near Chickaska, Grady County, OK, sampled on 17 December 2003. Sample size = 0.25 m^2, n = 24. Field 4—near Apache, Caddo County, OK, sampled on 18 December 2003. Sample size = 0.25 m^2, n = 24. Field 5—near Apache, Caddo County, OK, sampled on 19 December 2003. Sample size = 0.25 m^2, n = 18. GrHs Exp—greenhouse experiment, Potter County, Texas Agricultural Experiment Station at Bushland, TX, sampled on 23 May 2005. Sample size = 0.25 m^2, n = 10. GA, PGD, and VAPGD: greenbug abundance, percentage damage by greenbug estimated through assess, and visually assessed percentage damage by greenbug, respectively. S.E.: standard error of the mean; LCI: lower confidence interval; UCI: upper confidence interval.

where R_{719}, R_{873}, R_{509}, and R_{537} are the reflectance values of wavebands centered at 719, 873, 509, and 537 nm, respectively. S-PLUS 6.2 Professional for Windows (Insightful Inc., Seattle, WA) was used for correlation analyses to quantify the relationship between vegetation indices and damage by greenbugs.

3. Results and discussion

The descriptive statistics for greenbug abundance and damage are presented in Table 2. Greenbug abundance and damage to wheat varied widely across the fields and the greenhouse experiment, permitting a spectrum of damage severity in correlation analyses. The maximum (54,209 ± 7908/0.37 m^2) and minimum (191 ± 22/0.25 m^2) mean greenbug densities were found in the greenhouse experiment and Field 1, respectively. Field 2 had the second highest mean greenbug density (8603 ± 1411/1 m^2) followed by Field 5 (2443 ± 304/0.25 m^2), Field 3 (1646 ± 248/0.25 m^2), and Field 4 (291 ± 41/0.25 m^2) in descending order.

The most (73 ± 7/0.37 m^2) and least (13 ± 1/0.25 m^2) mean percent damage by greenbugs estimated through ASSESS were for the greenhouse experiment and Field 4. The visually assessed mean percent damage by greenbugs in the greenhouse experiment was slightly less (67 ± 9/0.37 m^2) with a greater standard error than that resulting from analysis with ASSESS (73 ± 7/0.37 m^2). The second greatest mean percent damage by greenbugs (47 ± 5/1 m^2) estimated through ASSESS was found in Field 2 followed by Field 1 (35 ± 2/0.25 m^2), Field 3 (24 ± 2/0.25 m^2), and Field 5 (17 ± 1/0.25 m^2) in descending order. Visually assessed mean percent damage by greenbugs in Field 2 was much greater (66 ± 4/1 m^2) with a lower standard error than ASSESS (47 ± 5/1 m^2). However, standard errors associated with mean percent damage by greenbugs seemed to be minimal across the fields. The statistics and data given in Table 2 indicated that using digital image analysis to estimate the percent damage by greenbugs at the canopy level is

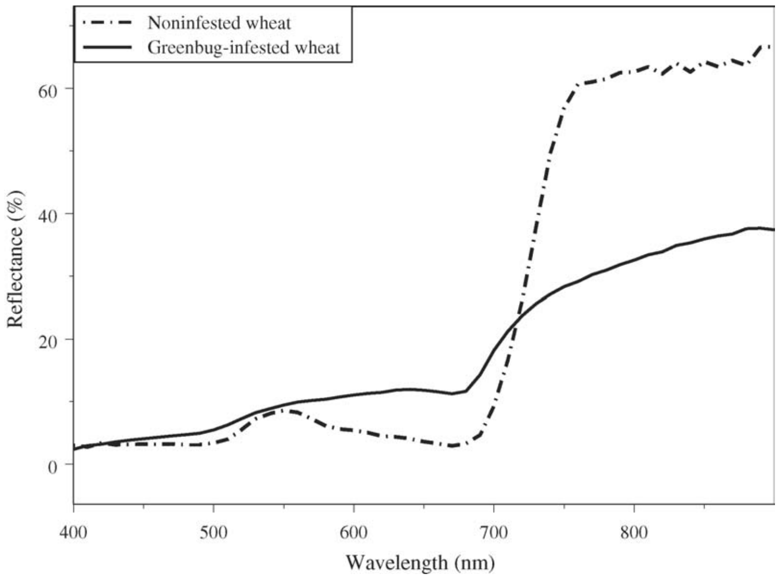

Fig. 2. Percentage spectral reflectance (400–900 nm range) of infested by greenbug (*Schizaphis graminum* (Rondani)) and noninfested winter wheat canopies collected in a greenhouse experiment at the Texas Agricultural Experiment Station facilities at Bushland, TX.

practical. Lamari (2002) indicated that ASSESS was designed to identify and quantify the background, leaf area, and chlorotic area in an image. Jones (2004) concluded that ASSESS was an ideal software package to rapidly and easily quantify certain types of plant disease.

The coefficient of variation (CV) = (standard deviation/mean) × 100 associated with damage by greenbugs estimated through ASSESS was greater (46) than visually assessed damage (25) suggesting better precision for Field 2. In contrast, the CV related to damage by greenbugs estimated through ASSESS was less (32) than visually assessed damage (43), suggesting less precision for the greenhouse experiment. High correlations ($r = 0.91$ and 0.93) were found between visually assessed and digitally estimated damage for Field 2 and greenhouse experiment, respectively. Richardson et al. (2001) used a digital camera to measure bermudagrass (*Cynodon dactylon* L.) cover and argued that digital image analysis was an effective method to quantify small differences in cover, generating accurate and reproducible data in addition to successfully removing evaluator bias and inherent error associated with visual ratings. Karcher and Richardson (2003) observed that the relative variance of the dark-green color index derived from digital images was significantly less than the variance associated with multiple raters when color of creeping bentgrass and zoysiagrass (*Zoysia japonica* Steud.) was quantified. Sherwood et al. (1983) reported that any visual disease quantification methods for purple leaf spot on orchardgrass (*Dactylis glomerata* L.) might be useful for ranking of plants varying widely in disease severity, but was unreliable for accurate quantification of disease progress and yield loss. Therefore, they suggested modification of the existing methods or development of a new technique that might use computerized analysis of video images as a potential system for assessing purple leaf spot. Niemira et al. (1999) discussed that the digital image analysis method could be a valuable tool in researching vulnerability of potato tubers to late blight.

Representative average reflectance spectra measured from the greenbug-infested and noninfested wheat canopies are presented in Fig. 2. It is clearly evident in Fig. 2 that the spectral characteristics of the wheat canopies were markedly affected by greenbug feeding. The reflectance of wheat canopies in the NIR region was significantly lower in contrast to a significant increase in the visible spectrum due to greenbug feeding (Mirik, unpublished data). The noninfested wheat canopies always captured more or reflected less light than the greenbug-infested wheat canopies in the range from 400 nm to the red edge shoulder at 720 nm.

Correlation analyses confirmed strong relationship between percent damage by greenbugs and spectral vegetation indices calculated with a spectral resolution of 7 nm (Table 3). It is interesting to note that most of vegetation indices compiled from the literature were negatively correlated with percent damage of greenbugs while $DSSI_1$ and $DSSI_2$ always were positively correlated (Table 3). The value of an index decreased with increasing damage severity, indicating a negative correlation. It is further interesting to note that among the vegetation indices from the literature, simple ratios

Table 3
Correlation coefficients associated with six spectral vegetation indices and percentage damage by greenbug (*Schizaphis graminum* (Rondani)) to wheat for five field and one greenhouse experiments

Index	r					
	ARI	$DSSI_1$	$DSSI_2$	IR − red difference	NDVI	PSSR
Field 1	-0.12^{ns}	0.97^{*}	0.78^{*}	-0.95^{*}	-0.28^{ns}	-0.44^{ns}
Field 2	-0.82^{*}	0.94^{*}	0.71^{*}	-0.93^{*}	-0.91^{*}	-0.66^{*}
Field 2[a]	-0.67^{*}	0.90^{*}	0.43^{ns}	-0.82^{*}	-0.82^{*}	-0.71^{*}
Field 3	-0.69^{*}	0.89^{*}	0.76^{*}	-0.55^{*}	-0.77^{*}	-0.83^{*}
Field 4	-0.54^{*}	0.72^{*}	0.82^{*}	-0.59^{*}	-0.47^{*}	-0.61^{*}
Field 5	-0.28^{ns}	0.35^{ns}	0.82^{*}	-0.34^{ns}	-0.43^{ns}	-0.13^{ns}
GrHs Exp	-0.98^{*}	0.88^{*}	0.71^{*}	-0.88^{*}	-0.96^{*}	-0.08^{ns}
GrHs Exp[a]	-0.90^{*}	0.88^{*}	0.82^{*}	-0.80^{*}	-0.89^{*}	-0.09^{ns}

R_{719}, R_{873}, R_{509}, R_{537}: reflectance values from wavebands centered at 719, 837, 509, and 537 nm with a spectral resolution of 7 nm, respectively. r: correlation coefficient; ns: nonsignificant at 0.05. Field 1—near Dumas, Moore County, TX, sampled on 21 November 2003. Sample size = 0.25 m^2, n = 8. Damage estimated through ASSESS. Field 2—near Chillicothe, Hardeman County, TX, sampled on 18 May 2005. Sample size = 1 m^2, n = 18. Damage estimated through ASSESS. Field 2[a]—damage visually assessed. Field 3—near Chickaska, Grady County, OK, sampled on 17 December 2003. Sample size = 0.25 m^2, n = 24. Damage estimated through ASSESS. Field 4—near Apache, Caddo County, OK, sampled on 18 December 2003. Sample size = 0.25 m^2, n = 24. Damage estimated through ASSESS. Field 5—near Apache, Caddo County, OK, sampled on 19 December 2003. Sample size = 0.25 m^2, n = 18. Damage estimated through ASSESS. GrHs Exp, greenhouse experiment—Potter County, Texas Agricultural Experiment Station at Bushland, TX, sampled on 23 May 2005. Sample size = 0.37 m^2, n = 10. Damage estimated through ASSESS. GrHs Exp[a]—damage visually assessed. ARI: Anthocyanin Reflectance Index $((1/R_{628}) - (1/R_{747}))$ modified from Gitelson et al. (2001). $DSSI_1$: Damage Sensitive Spectral Index$_1$ $(R_{719} - R_{873} - R_{509} - R_{537})/((R_{719} - R_{873}) + (R_{509} - R_{537}))$ (this work). $DSSI_2$: Damage Sensitive Spectral Index$_2$ $(R_{747} - R_{901} - R_{537} - R_{572})/((R_{747} - R_{901}) + (R_{537} - R_{572}))$ (this work). IR − red difference $(R_{789} - R_{663})$ developed by Tucker (1979). NDVI: Normalized Difference Vegetation Index $(R_{754} - R_{712})/(R_{754} + R_{712})$ developed by Gamon and Surfus (1999). PSSR: Pigment Specific Simple Ratio (R_{775}/R_{747}) developed by Blackburn and Steele (1999).

* Significant at 0.05.

provided better relationships with percent damage by greenbugs than did the others with one exception. The NDVI of Gamon and Surfus (1999) and Difference Vegetation Index of Tucker (1979) showed equal relationships (r = −0.82) with visually assessed percent damage by greenbugs collected in Field 2. The performance of simple ratios found in this study agreed with the results of Yang et al. (2005) who investigated the threshold days on which the significant differences in spectral reflectance between greenbug-infested and noninfested wheat canopies were revealed in a time series experiment. They argued that simple ratio-based vegetation indices were more sensitive to greenbug abundance than were the others. For example, the NDVI and Soil Adjusted Vegetation Index (Huete, 1988) did not show significant sensitivity to greenbug abundance.

The correlation coefficients between percent damage by greenbugs and vegetation indices ranged from −0.98 to −0.08 for the greenhouse experiment (Table 3). The $DSSI_1$ produced consistently greater correlations with percent damage by greenbugs collected in Fields 1–3, whereas $DSSI_2$ worked substantially better for Fields 4–5 than did any other index examined. The Anthocyanin Reflectance Index showed the best performance (r = −0.98) for the greenhouse experiment although $DSSI_1$ (r = 0.88) and $DSSI_2$ (r = 0.71) also were closely correlated to percent damage by greenbugs in the same experiment. The visually assessed percent damage by greenbugs in Field 2 (r = 0.90) and the greenhouse experiment (r = −0.96) had slightly less correlations with vegetation indices when compared to estimates of ASSESS for Field 2 (r = 0.94) and the greenhouse experiment (r = −0.98). These results are somewhat in agreement with Adamsen et al. (1999) who used a digital camera and a hand-held radiometer to measure wheat senescence. The authors found a high correlation (R^2 = 0.962) between green and red (G/R) values calculated from digital images and NDVI derived from a radiometer, and stated that digital imaging seems useful for quantifying the senescence of crop canopies.

In general, the correlations between percent damage by greenbugs and vegetation indices were less (r = 0.89, 0.82, and 0.82) for Fields 3–5, respectively, than Fields 1 (r = 0.97) and 2 (r = 0.94), and the greenhouse experiment (r = −0.98). Perhaps one reason for the lower correlations for Fields 3–5 was that damage severity varied from minimal with a mean of 13% in Field 4 to slight with a mean of 24% in Field 3 (Table 2). Zhang et al. (2003) tested the capacity of hyperspectral image data to distinguish the severity of late blight disease from stage 1 (slight) to stage 4 (severe) in tomato. The authors concluded that the diseased vegetation at stages 1–2 was difficult to separate from the healthy plants while tomatoes infected by late blight disease at stages 3–4 were separated from noninfected tomatoes. Discrimination of healthy rice plants from ones lightly infected (<20) by rice sheath blight was difficult because of the high overlap in the estimated image indices, whereas identification was more accurate when disease was moderate to severe (Qin and Zhang, 2005). Another potential reason for lesser correlations for Fields 3–5 was the noise added by reflectance of a large soil background. During the data collection, Field 5 had the most exposed soil in each of the 18, 0.25-m^2 plots followed by Fields 4–3. The greenhouse experiment presented more evidence that data collected in a controlled environment produced the greatest correlation among the sites. This implies that variations in the greenhouse were much less than those in the field. Hence, it seems that $DSSI_2$ tends to enhance the contrast between vegetation and soil and works better for less severe damage, while $DSSI_1$ is more sensitive to more severe damage in wheat. The original version of these indices correlated well with the vegetation fraction of wheat (Gitelson et al., 2002) but was not among the top six indices listed in Table 3 for fields in this work.

4. Conclusions

The authors are unaware of any studies attempting to correlate spectral vegetation indices to damage by greenbugs or any other damage estimated through digital image analysis. However, correlating the estimates of leaf area index, a central biophysical variable influencing the land surface processes (Wang et al., 2005), through various leaf area index meters to spectral vegetation indices has been a well established practice in remote sensing studies (Anderson et al., 2004; Hu et al., 2004; Walthall et al., 2004; Schlerf et al., 2005 among many others). Another comparison that has long been used is the relationship between vegetation indices and plant chlorophyll concentration measured by spectrophotometers after chemical extraction or chlorophyll meters (Rosemary et al., 1999; Broge and Mortensen, 2002).

The results of this study indicated that remotely sensed data recorded by a hyperspectral spectrometer and a digital camera have the potential to aid in monitoring damage by greenbugs in wheat growing under field conditions. However, although the spectral vegetation indices tested gave strong correlations, there was no single best index for damage by greenbugs in all situations. It seems that the sensitivity of an index differs because of environmental and ecological variability from one place to another. Therefore, no single index with the same spectral bands was found to be correlated with damage by greenbugs in this research. It also appears that there is no single spectral index applicable for all surface characteristics including stress quantification in plants. This implies that a few spectral vegetation indices can be calculated and associated with greenbug damage in fields where the variability in soil, vegetation, and weather differs from place to place. In this study, $DSSI_1$, $DSSI_2$, SR, and NDVI were strongly related to damage by greenbugs; thus, they are recommended for studies of damage by aphids in wheat.

Digitally estimated, as well as visually assessed, damage by greenbugs correlated well with vegetation indices. Digital image analysis may be an alternative to visual techniques, even though there were no substantial differences in correlation coefficients between visually assessed versus digitally estimated damage by greenbugs. However, digital data have an advantage because they can be reproduced, stored, and used at a later time as historical documents of vegetation status. Strong correlations between spectral indices and damage by greenbugs suggest that hyperspectral imaging sensors can be used as a quick, nondestructive, repeatable, and cost-effective technique to detect aphid and other types of damage in wheat. This study was a first step to use reflectance measurements and digital image analysis to estimate damage by greenbugs. More studies are needed to confirm the results found. Additionally, future research using image data taken from aircraft or satellite platforms is also needed to expand the study to the whole field or landscape level.

Acknowledgements

Our special thanks go to Karl Steddom and Roxanne Bowling for their help and beneficial discussion. We are thankful to Vanessa Carney, Johnny Bible, Robert Villarreal, David Jones, Timothy Johnson, Steven South, Traci Rowland, and Satishreddy Ambati for their technical assistance. This project was funded by the USDA-ARS Areawide Pest Management Program, Project Number: 500-44-012-00.

References

Adams, M.L., Norvell, W.A., Philpot, W.D., Peverly, J.H., 2000. Spectral detection of micronutrient deficiency in ‘Bragg’ soybean. Agron. J. 92, 261–268.

Adamsen, F.J., Pinter Jr., P.J., Barnes, E.M., LaMorte, R.L., Wall, G.W., Leavitt, S.W., Kimball, B.A., 1999. Measuring wheat senescence with a digital camera. Crop Sci. 39, 719–724.

Anderson, M.C., Neale, C.M.U., Li, F., Norman, J.M., Kustas, W.P., Jayanthi, H., Chavez, J., 2004. Upscaling ground observations of vegetation water content, canopy height, and leaf area index during SMEX02 using aircraft and Landsat imagery. Remote Sens. Environ. 92, 447–464.

Aquino, V.M., Shokes, F.M., Berger, R.D., Gorbet, D.W., Kucharek, T.A., 1992. Relationships among late leafspot, healthy leaf area duration, canopy reflectance, and pod yield of peanut. Phytopathology 82, 546–552.

Bawden, F.C., 1933. Infra-red photography and plant virus disease. Nat. (Lond.) 132, 168.

Blackburn, G.A., Steele, C.M., 1999. Towards the remote sensing of matorral vegetation physiology: relationships between spectral reflectance, pigments, and biophysical characteristics of semiarid bushland canopies. Remote Sens. Environ. 70, 278–292.

Blazquez, C.H., Edwards, G.J., 1986. Spectral reflectance of healthy and diseased watermelon leaves. Ann. Appl. Biol. 108, 243–249.

Bouman, B.A.M., 1995. Crop modeling and remote sensing for yield prediction. Neth. Agric. Sci. 43, 143–161.

Broge, N.H., Mortensen, J.V., 2002. Deriving green crop area index and canopy chlorophyll density of winter wheat from spectral reflectance data. Remote Sens. Environ. 81, 45–57.

Carter, G.A., Seal, M.R., Haley, T., 1998. Airborne detection of southern pine beetle damage using key spectral bands. Can. J. For. Res. 28, 1040–1045.

Ceccato, P., Gobron, N., Flasse, S., Pinty, B., Tarantola, S., 2002. Designing a spectral index to estimate vegetation water content from remote sensing data: part 1 theoretical approach. Remote Sens. Environ. 82, 188–197.

Díaz-Lago, J.E., Stuthman, D.D., Leonard, K.J., 2003. Evaluation of components of partial resistance to oat crown rust using digital image analysis. Plant Dis. 87, 667–674.

Diéguez-Uribeondo, J., Förster, H., Adaskaveg, J.E., 2003. Digital image analysis of internal light spots of appressoria of *Colletotrichum acutatum*. Phytopathology 93, 923–930.

Fensholt, R., Sandholt, I., 2003. Derivation of a shortwave infrared water stress index from MODIS near- and shortwave infrared data in a semiarid environment. Remote Sens. Environ. 87, 111–121.

Gamon, J.A., Surfus, J.S., 1999. Assessing leaf pigment content and activity with a reflectometer. New Phytol. 143, 105–117.

Gao, B.-C., 1996. NDWI—a normalized difference water index for remote sensing of vegetation liquid water from space. Remote Sens. Environ. 58, 257–266.

Gitelson, A.A., Merzlyak, M.N., Chivkunova, O.B., 2001. Optical properties and nondestructive estimation of anthocyanin content in plant leaves. J. Photochem. Photobiol. 74, 38–45.

Gitelson, A.A., Kaufman, Y.J., Stark, R., Rundquist, D., 2002. Novel algorithms for remote estimation of vegetation fraction. Remote Sens. Environ. 80, 76–87.

Guan, J., Nutter Jr., F.W., 2002. Relationships between percentage defoliation, dry weight, percentage reflectance, leaf-to-stem ratio, and green leaf area index in the alfalfa leaf spot pathosystem. Crop Sci. 42, 1264–1273.

Horst, G.L., Engelke, M.C., Meyers, W., 1984. Assessment of visual evaluation techniques. Agron. J. 76, 619–622.

Hu, B., Qian, S.-N., Haboudane, D., Miller, J.R., Hillinger, A.B., Tremblay, N., Pattey, E., 2004. Retrieval of crop chlorophyll content and leaf area index from decompressed hyperspectral data: the effects of data compression. Remote Sens. Environ. 92, 139–152.

Huete, A.R., 1988. A soil-adjusted vegetation index (SAVI). Remote Sens. Environ. 25, 295–309.

Hunt Jr., E.R., Rock, B.N., 1989. Detection of changes in leaf water content using near- and middle-infrared reflectances. Remote Sens. Environ. 30, 43–54.

Jones, D., 2004. Remote detection of wheat streak mosaic and nitrogen deficiency and their effects on hard red winter wheat. M.S. Thesis. West Texas A&M University, Canyon, TX.

Jordan, C.J., 1969. Derivation of leaf-area index from quality of light on the forest floor. Ecology 50, 663–666.

Karcher, D.E., Richardson, M.D., 2003. Quantifying turfgrass color using digital image analysis. Crop Sci. 43, 943–951.

Kim, Y.S., Reid, J.F., Hansen, A., Zhang, Q., 2000. On-field crop stress detection system using multi-spectral imaging sensor. Agric. Biosyst. Eng. 2, 88–94.

Kobayashi, T., Kanda, E., Kitada, K., Ishiguro, K., Torigoe, Y., 2001. Detection of rice panicle blast with multispectral radiometer and the potential of using airborne multispectral scanners. Phytopathology 91, 316–323.

Kruse, J.K., Christians, N.E., Chaplin, M.H., 2004. Nitrogen Deficiencies in Creeping Bentgrass can be Identified through Remote Sensing, available online at http://turfgrass.hort.iastate.edu/pubs/turfrpt/2004/pdf/54-56RemoteSensing.pdf (accessed on 02.09.2005).

Lamari, L., 2002. ASSESS: Image Analysis Software for Plant Disease Quantification. The American Phytopathological Society Press, St. Paul, MN.

Laudien, R., Bareth, G., Doluschitz, R., 2004. Comparison of remote sensing based analysis of crop disease by using high resolution multispectral and hyperspectral data—case study: rhizoctonia solani in sugar beet. In: Proceedings of 12th International Conference on Geoinformatics—Geospatial Information Research: Bridging the Pacific and Atlantic University of Gävle, Sweden, pp. 670–676.

Leckie, D.G., Cloney, E., Joyce, S.P., 2005. Automated detection and mapping of crown discoloration caused by jack pine budworm with 2.5 m resolution multispectral imagery. Int. J. Appl. Earth Observation Geoinf. 7, 61–77.

Lelong, C.C.D., Pinet, P.C., Poilvé, H., 1998. Hyperspectral imaging and stress mapping in agriculture: a case study on wheat in Beauce (France). Remote Sens. Environ. 66, 179–191.

Malthus, T.M., Madeira, A.C., 1993. High resolution spectroradiometry: spectral reflectance of field bean leaves infected by *Botrytis fabae*. Remote Sens. Environ. 45, 107–116.

Mariotti, M., Ercoli, L., Masoni, A., 1996. Spectral properties of iron-deficient corn and sunflower leaves. Remote Sens. Environ. 58, 282–288.

Merzlyak, M.N., Gitelson, A.A., Chivkunova, O.B., Rakitin, V.Y., 1999. Non-destructive optical detection of pigment changes during leaf senescence and fruit ripening. J. Plant Physiol. 106, 135–141.

Moran, M.S., Clarke, T.R., Inoue, Y., Vidal, A., 1994. Estimating crop water deficit using the relationship between surface-air temperature and spectral vegetation index. Remote Sens. Environ. 49, 246–263.

Muhammed, H.H., 2004. Characterizing and estimating fungal disease severity in wheat. In: Swedish Society for Automated Image Analysis Symposium—SSBA 2004, Ångströmlaboratoriet, Uppsala University, Centre for Image Analysis, Sweden, pp. 194–198.

Muhammed, H.H., Larsolle, A., 2003. Feature vector based analysis of hyperspectral crop reflectance data for discrimination and quantification of fungal disease severity in wheat. Biosyst. Eng. 86, 125–134.

Newton, A.C., Hackett, C.A., Lowe, R., Wale, S.J., 2004. Relationship between canopy reflectance and yield loss due to disease in barley. Ann. Appl. Biol. 145, 95–106.

Niemira, B.A., Kirk, W.W., Stein, J.M., 1999. Screening for late blight susceptibility in potato tubers by digital analysis of cut tuber surfaces. Plant Dis. 83, 469–473.

Nilsson, H.-E., 1995. Remote sensing and image analysis in plant pathology. Annu. Rev. Phytopathol. 15, 489–527.

Nilsson, H.-E., Johnsson, L., 1996. Hand-held radiometry of barley infected by barley stripe disease in a field experiment. J. Plant Dis. Prot. 103, 517–526.

Nutter Jr., F.W., Littrell, R.H., 1996. Relationships between defoliation, canopy reflectance and pod yield in the peanut–late leafspot pathosystem. Crop. Prot. 15, 135–142.

Nutter Jr., F.W., Gleason, M.L., Jenco, J.H., Christians, N.C., 1993. Assessing the accuracy, inter-rater repeatability and inter-rater reliability of disease assessment systems. Phytopathology 83, 806–812.

Nutter Jr., F.W., Guan, J., Gotlieb, A.R., Rhodes, L.H., Grau, C.R., Sulc, R.M., 2002. Quantifying alfalfa yield losses caused by foliar diseases in Iowa, Ohio, Wisconsin, and Vermont. Plant Dis. 86, 269–277.

Peñuelas, J., Isla, R., Filella, I., Araus, J.L., 1997. Visible and near-infrared reflectance assessment of salinity effects on barley. Crop Sci. 37, 198–202.

Qin, Z., Zhang, M., 2005. Detection of rice sheath blight for in-season disease management using multispectral remote sensing. Int. J. Appl. Earth Observation Geoinf. 7, 115–128.

Raikes, C., Burpee, L.L., 1998. Use of multispectral radiometry for assessment of *Rhizoctonia* blight in creeping bentgrass. Phytopathology 88, 446–449.

Read, J.J., Tarpley, L., McKinion, J.M., Reddy, K.R., 2002. Narrow-waveband reflectance ratios for remote estimation of nitrogen status in cotton. J. Environ. Qual. 31, 1442–1452.

Richardson, M.D., Karcher, D.E., Purcell, L.C., 2001. Quantifying turfgrass cover using digital image analysis. Crop Sci. 41, 1884–1888.

Riedell, W.E., Blackmer, T.M., 1999. Leaf reflectance spectra of cereal aphid-damaged wheat. Crop Sci. 39, 1835–1840.

Rosemary, A.J., Cutler, M.E.J., Curran, P.J., 1999. Estimating canopy chlorophyll concentration from field and airborne spectra. Remote Sens. Environ. 68, 217–224.

Rouse, J.W., Haas, R.H., Schell, J.A., Deering, D.W., 1973. Monitoring vegetation systems in the Great Plains with ERTS. In: Proceedings, Third ERTS Symposium, NASA Sp-351, vol. 1, Washington, DC, pp. 309–317.

Schlerf, M., Atzberger, C., Hill, J., 2005. Remote sensing of forest biophysical variables using HyMap imaging spectrometer data. Remote Sens. Environ. 95, 177–194.

Serrano, L., Peñuelas, J., Ustin, S.L., 2002. Remote sensing of nitrogen and lignin in Mediterranean vegetation from AVIRIS data: decomposing biochemical from structural signals. Remote Sens. Environ. 81, 355–364.

Sherwood, R.T., Berg, C.C., Hoover, M.R., Zeiders, K.E., 1983. Illusions in visual assessment of Stagonaspora leaf spot of orchardgrass. Phytopathology 73, 173–177.

Skogley, C.R., Sawyer, C.D., 1992. Field research. In: Waddington, D.V., Carrow, R.N., Shearman, R.C. (Eds.), Turfgrass. Agron. J. 32, 653–688.

Steddom, K., Heidel, G., Jones, D., Rush, C.M., 2003. Remote detection of Rhizomania in sugar beet. Phytopathology 93, 720–726.

Steddom, K., McMullen, M., Schatz, B., Rush, C.M., 2004. Assessing foliar disease of wheat image analysis. In: The 2004 Summer Crops Field Day at Bushland, TX Sponsored by the Cooperative Research, Education & Extension Team (CREET), Bushland, TX, pp. 32–38.

Steddom, K., Jones, D., Rush, C., 2005a. A Picture is Worth a Thousand Words, available online at http://www.apsnet.org/online/feature/remote/ (accessed on 02.09.2005).

Steddom, K., Bredehoeft, M.W., Khan, M., Rush, C.M., 2005b. Comparison of visual and multispectral radiometric disease evaluations of cercospora leaf spot of sugar beet. Plant Dis. 89, 153–158.

Toler, R.W., Smith, B.D., Harlan, J.C., 1981. Use of aerial color infrared to evaluate crop disease. Plant Dis. 65, 24–31.

Trenholm, L.E., Carrow, R.N., Duncan, R.R., 1999. Relationship of multispectral radiometry data to qualitative data in turfgrass research. Crop Sci. 39, 763–769.

Tucker, C.J., 1979. Red and photographic infrared linear combinations for monitoring vegetation. Remote Sens. Environ. 8, 127–150.

Turner, A.V., Martin, S.B., Camberato, J.J., 2004. Image Analysis to Quantify Foliage Damage to Turfgrass, available online at http://virtual.clemson.edu/groups/turfornamental/sctop/turfsec/plpanem/plpanem6.htm (accessed on 02.09.2005).

Walthall, C., Dulaney, W., Anderson, M., Norman, J., Fang, H., Liang, S., 2004. A comparison of empirical and neural network approaches for estimating corn and soybean leaf area index from Landsat ETM+ imagery. Remote Sens. Environ. 92, 465–474.

Wang, Q., Adiku, S., Tenhunen, J., Granier, A., 2005. On the relationship of NDVI with leaf area index in a deciduous forest site. Remote Sens. Environ. 94, 244–255.

Webster, J., Treat, R., Morgan, L., Elliott, N., 2000. Economic Impacts of the Russian Wheat Aphid and Greenbug in the Western United States 1993–94, 1994–95, and 1997–98. U.S. Department of Agriculture, ARS Service Report PSWCRL Re 00-001.

Yang, Z., Rao, M.N., Elliott, N.C., Kindler, S.D., Popham, T.W., 2005. Using ground-based multispectral radiometry to detect stress in wheat caused by greenbug (Homoptera: Aphididae) infestation. Comp. Electr. Agric. 47, 121–135.

Yoshioka, H., Miura, T., Huete, A.R., Ganapol, B.D., 2000. Analysis of vegetation isolines in red–NIR reflectance space. Remote Sens. Environ. 74, 313–326.

Zadoks, J.C., Chang, T.T., Konzak, C.F., 1974. A decimal code for the grown stages of cereals. Weed Res. 14, 415–421.

Zhang, M., Qin, Z., Liu, X., Ustin, S.L., 2003. Detection of stress in tomatoes induced by late blight disease in California, USA, using hyperspectral remote sensing. Int. J. Appl. Earth Observation Geoinf. 4, 295–310.